Minimax Theory and its Applications
Volume 11 (2026), No. 4s, 509 to 518

Topological solution characterization of feasible regions in complex engineering optimization problems with nonlinear constraints

Dr.A. Santhosh Prakash[1], Dr. Vikas Dilliwar[2], Dr.J. Abdul Bari[3], Dr. T. V. Ambuli[4], Ashutosh Pandey[5], Kotnani Pvsr Vinay Kumar[6]

[1]Associate Professor, Department of Mechanical Engineering, J.J. College of Engineering and Technology, Tiruchirappalli, Tamil Nadu, India. santhoshprakasha@jjcet.ac.in, https://orcid.org/0009-0009-3835-2638

[2]Associate Professor, Department of Computer Science and Engineering, Rungta College of Engineering and Technology, Rungta International Skills University, Bhilai, Chhattisgarh, India. vikas.dilliwar@rungta.org, https://orcid.org/0000-0003-4656-4410

[3]Associate Professor, Department of Civil Engineering, K.S. Rangasamy College of Technology, Namakkal, Tamil Nadu, India. abdulbari@ksrct.ac.in, https://orcid.org/0000-0002-6502-296X

[4]Associate Professor and Head, Department of Commerce, Faculty of Science and Humanities, SRM Institute of Science and Technology, Ramapuram, Chennai, Tamil Nadu, India. ambuli70@gmail.com, https://orcid.org/0000-0003-3853-182X

[5]Assistant Professor, Kalinga University, Naya Raipur, Chhattisgarh, India. ku.ashutoshpandey@kalingauniversity.ac.in, https://orcid.org/0009-0004-7931-0091

[6]Department of Mechanical, Ramachandra College of Engineering, Eluru, Andhra Pradesh, India. vk281976@rcee.ac.in, https://orcid.org/0000-0002-2068-2040

Abstract:

In structural design, fluid-structure interaction, and aerodynamic configuration, solving complex engineering optimization problems often involves high-dimensional, highly nonlinear, and non-convex constraints, making it impossible for conventional optimization methods, such as gradient descent and interior-point strategies, to traverse between different regions of the feasible (i.e., feasible) solution set. In most analyses of feasible regions, only local geometry is leveraged, including properties like convexity, star-shapedness, and Karush-Kuhn-Tucker stationarity, therefore neglecting the global topological structure of the feasible region. The present paper proposes a general topological framework for mapping non-linear feasible sets onto CW complexes and stratified manifolds, introduces the precise criteria for contractibility, homotopy equivalence, and path-connectedness of the feasible region, and establishes two theorems connecting specific homotopy-theoretic invariants of the topology with the global convergence of optimization processes. In particular, the presented method employs Betti numbers and persistent homology to estimate the number of connected components and independent loops induced by non-linear equality and inequality constraints, and applies Morse inequalities to derive lower bounds on the total number of stationary points. Sample calculations performed on the truss optimization problem with non-convex characteristics and the synthesis of kinematic mechanisms demonstrate that having four disconnected regions the single-start gradient descent method will, probably, succeed in finding the global optimum 24% of the time, while the interior-point technique will only yield a 29% success rate. At the same time, the topology-aware multi-start algorithm achieving 90% of success under the same condition needed on, average, 51% less iterations than the interior-point strategy. In addition, the persistent homology allows for identifying actual topological voids at the filtration values that are over an order of magnitude larger than the sampling noise error. The above results show that global topological

characterization of feasible region is both a mathematically rigorous and practically useful approach to tackle problems related to failure of engineering design optimization processes.

Keywords: Topological optimization, feasible region connectivity, algebraic topology, Betti numbers, persistent homology, nonlinear constrained optimization.

1. Introduction

Complicated engineering optimization problems, ranging from structural weight reduction to fluid-structure interaction and aerodynamic design, are generally characterized by complicated many-dimensional nonlinear non-convex constraints giving way to feasible regions that present a set of disconnected components and non-smooth boundaries as well as topological obstacles within the search space. Standard gradient-based approaches and interior point techniques are often applied to these types of problems, while feasibility-guided constraint handling techniques have been developed to improve these methods' performance with complex constraint systems (Jan et al., 2021); however, still tend to fail whenever the feasible region in itself does not have a continuous connection between an arbitrary start point and the global solution, a situation that cannot be remedied by local constraint handling methods.

Formulations of nonlinear topology optimization under constraints relating to temperature demonstrate the ability of strongly coupled physical constraints to result in highly nonconvex and topologically complex feasible domains in even the most established field of engineering, while multiobjective lattice topology optimization for lightweight structures results in a feasible region that cannot be captured by relying solely on local sensitivity analysis (Zhuang et al., 2021). Topology optimization subject to local stress constraints has indicated that the set of active constraints can vary discontinuously in the design space, while formulations of equilibrium problems solved using subgradient extrapolation methods in generic Banach spaces indicate that convergence properties of iterative techniques depend on the structural characteristics of the respective feasible set or equilibrium set, rather than on their local smoothness (Senhora et al., 2023; Thomas & Suchitra, 2026; Jolaoso & Aphane, 2022).

Most of today's research into engineering optimization feasible sets concentrates on the geometric aspects of these objects such as their convexity and star-shapedness or other familiar local analytical optimality criteria (for instance, Karush-Kuhn-Tucker conditions), yet without any references to global topological characteristics (like connectedness, homology groups, Betti numbers, or persistent homology), which is unreasonable, as such a lack of rigorous topological insights prevents rigorous insights into the reasons behind why optimization efforts get stuck and fail to pass from one feasible region to another. The significance of this point is determined by the fact that metaheuristic and population-based methods, including genetic algorithms, swarm intelligence, and nature-inspired optimization techniques, have been successfully developed and widely used in the engineering field for various optimization cases (Rajan & Shanthi, 2015; Şenol et al., 2024). Research in this area proves that different recent metaheuristic approaches to engineering optimization will perform quite poorly if the feasible set consists of disconnected regions (Yang, 2024; Altay et al., 2023). In addition, among solutions proposed to tackle this problem of performance degradation due to restricted feasible regions, constraint relaxation strategy for multi-objective optimization is also the one that has been used in practice (Sun et al., 2022; Houssein et al., 2025).

The rapidly-growing collection of metaheuristic algorithms such as modified sea horse optimizer (Hashim et al., 2024), an overview of comparisons of constrained mechanical design problems (Gupta et al., 2021), population-based structural engineering optimization (Kashani et al., 2022), hybrid bat-cuckoo search techniques for
large-scale constrained design (Pathak & Srivastava, 2022), the flow direction method (Karami et al., 2021), growth optimizer (Zhang et al., 2023), enhanced version of cuckoo search algorithm (Cuong-Le et al., 2021), along with Lotus Effect optimization method (Dalirinia et al., 2024), has been recently established to address the difficulty of designing in non-convex engineering design environments with many constraints, but it has not yet been linked to a topological explanation for the geometry of the feasible regions causing such difficulty.

This paper outlines three main contributions that fill this gap: (i) the development of a solid mathematical methodology which transforms non-linear feasible domains into topological manifolds and CW complexes; (ii) the statement of exact topological relations such as connectedness, contractibility, and homotopy equivalence for the feasible domain which leads to formal statements relating homotopic invariants and global convergence bounds of the optimization process; (iii) the demonstration of the correctness of such topological classifications with numerical examples reflecting the results of applications of non-convex structural trusses and kinematic mechanisms design problems which confirm that topology-aware optimization can significantly outperform the classical single-star approaches on feasible domains with non-trivial connectivity.

The remainder of the paper proceeds as follows. Section II formulates the general constrained optimization problem and the topological preliminaries required for the subsequent analysis. Section III develops the topological characterization of the feasible region, including manifold structure, connectivity, homotopy analysis, and Betti number computation. Section IV analyzes the impact of feasible-region topology on optimization dynamics, including Morse-theoretic bounds on local minima multiplicity and a global convergence theorem. Section V applies the framework to two benchmark engineering optimization problems and reports the resulting numerical results. Section VI discusses theoretical comparisons, computational complexity, and limitations. Section VII concludes the paper.

2. Mathematical formulation and preliminaries

2.1. Problem definition

The general constrained optimization problem considered throughout is defined by the objective function and constraint set given in Equation (1):

$$\min_{x \in X \subseteq \mathbb{R}^n} f(x) \quad \textit{subject to} \quad g_i(x) \leq 0 \quad (i = 1, \dots, m), \quad h_j(x) = 0 \quad (j = 1, \dots, p), \tag{1}$$

with corresponding feasible region Ω, defined in Equation (2):

$$\Omega = \{x \in X : g_i(x) \leq 0 \textit{ for all } i,\ h_j(x) = 0 \textit{ for all } j\} \tag{2}$$

2.2. Topological foundations

The feasible region Ω, defined in Equation (2), is regarded as a subset of Euclidean space $\mathbb{R}^n$ endowed with the standard metric topology induced by the Euclidean norm. A subset A of Ω is path-connected if any two points of A can be joined by a continuous path lying entirely within A; Ω is compact if it is closed and bounded; the boundary $\partial\Omega$ consists of points every neighborhood of which intersects both Ω and its complement, and the interior $\mathrm{Int}(\Omega)$ consists of points admitting a neighborhood contained entirely in Ω. The active constraint surfaces $\{x : g_i(x) = 0\}$ from Equation (1) are said to satisfy a regularity or transversality condition at a point x if the gradients of the active constraints at x are linearly independent, which guarantees that the boundary $\partial\Omega$ is locally a smooth manifold of codimension equal to the number of active constraints near that point.

Morse theory relates the topology of sublevel sets $\Omega_c = \{x \in \Omega : g(x) \leq c\}$, for a scalar constraint or auxiliary function g, to the critical points of g, that is, points at which $\nabla g(x) = 0$. The Morse index of a non-degenerate critical point is the number of negative eigenvalues of the Hessian of g at that point, and the topology of Ω_c changes only as c passes through a critical value, with the nature of the change determined by the Morse index of the corresponding critical point.

3. Topological characterization of the feasible region

3.1. Manifold structure and boundary topology

Under the regularity condition of Section 2.2, the feasible region Ω defined by Equation (2) constitutes a topological manifold with boundary, or more generally a stratifiable set, on the subset of X where the active constraint gradients remain linearly independent. Non-smooth boundary intersections occur precisely where the transversality condition fails, that is, where two or more active constraint surfaces meet tangentially or where their gradients become linearly dependent; at such points, Ω fails to be a manifold with boundary in the classical sense and must instead be treated as a stratified set, decomposed into strata of varying dimension corresponding to the number and configuration of simultaneously active constraints.

3.2. Connectivity and homotopy analysis

A non-convex feasible region generally decomposes into a finite union of path-connected components:

$$\Omega = \bigcup_{k=1}^{K} \Omega_k \tag{3}$$

where each component Ω_k in Equation (3) is maximal path-connected and satisfies $\Omega_k \cap \Omega_l = \emptyset$ for $k \neq l$. The fundamental group $\pi_1(\Omega_k)$ of each component classifies holes, voids, and tunnels induced by nonlinear equality

and inequality constraints acting jointly on that component: a trivial fundamental group indicates that every loop in Ω_k is contractible to a point within Ω_k, while a non-trivial fundamental group indicates the presence of at least one non-contractible loop, corresponding physically to a region of infeasible design space entirely surrounded by feasible configurations.

Theorem 1 (Sublevel set inclusion and topological change under constraint deformation)

Statement. Let $\{g_i(x;t)\}_{t\in[0,1]}$ be a smooth one-parameter family of constraint functions deforming the feasible region $\Omega(t) = \{x: g_i(x;t) \leq 0 \text{ for all } i\}$ defined analogously to equation (2). If no critical point of any $g_i(\cdot;t)$ crosses the level 0 as t varies over an interval $[t_1, t_2]$, then $\Omega(t_1)$ and $\Omega(t_2)$ are homotopy equivalent, and in particular have identical Betti numbers $\beta_k\big(\Omega(t_1)\big) = \beta_k\big(\Omega(t_2)\big)$ for all k. Conversely, if a critical point of Morse index λ crosses the level 0 at some $t^* \in [t_1, t_2]$, the homotopy type of $\Omega(t)$ changes at $t = t^*$ by the attachment of a λ-cell, altering β_λ by exactly one (up to cancellation with an adjacent index $\lambda \pm 1$ feature).

Proof sketch. The forward direction follows from the standard Morse-theoretic result that the sublevel sets of a smooth function are homotopy equivalent across any interval of parameter values containing no critical value, since a deformation retraction of $\Omega(t_2)$ onto $\Omega(t_1)$ can be constructed by flowing along the negative gradient of the deforming constraint function whenever no critical point crosses the boundary level during the interval. The converse follows from the Morse Lemma applied at the crossing critical point: in a neighborhood of a non-degenerate critical point of index λ, the sublevel set changes homotopy type precisely by the attachment of a λ-cell as the level passes through the critical value, which by the long exact sequence of the pair $\big(\Omega(t^* + \delta), \Omega(t^* - \delta)\big)$ in homology alters the rank of H_λ, and hence β_λ, by exactly one, unless this new generator is immediately cancelled against an adjacent generator in the persistent homology sense, which is precisely the topological noise filtered out by the persistence analysis.

3.3. Algebraic topology and betti numbers

The homology groups $H_k(\Omega;\mathbb{R})$ and their ranks, the Betti numbers $\beta_k(\Omega) = \dim(H_k(\Omega;\mathbb{R}))$, quantify the number of k-dimensional voids in the feasible region Ω of Equation (2): β_0 counts the number of path-connected components K shown in Equation (3), β_1 counts independent one-dimensional loops or tunnels, and β_2 counts enclosed two-dimensional voids, with higher β_k quantifying higher-dimensional analogues. Because Ω is generally known only through a finite sample of feasible points obtained by constraint satisfaction sampling, persistent homology is used to compute Betti numbers robustly: a nested filtration of simplicial complexes is built over the sampled point cloud as a scale parameter ε increases, and topological features (connected components, loops, voids) are tracked across the filtration, with each feature assigned a birth and death filtration value. Features with long persistence (large death-minus-birth interval) are interpreted as genuine geometric characteristics of the feasible region, while short-lived features are treated as topological noise arising from finite sampling density.

4. Impact of topology on optimization dynamics and feasibility trajectories

4.1. Continuous feasible paths and search dynamics

A continuous feasible path between an initial point $x_0 \in \Omega$ and a local or global minimizer $x^* \in \Omega$ of Equation (1) exists if and only if x_0 and x^* lie in the same path-connected component Ω_k of the decomposition given in Equation (3). When Ω is disconnected ($\beta_0 > 1$) or exhibits non-trivial fundamental group ($\pi_1(\Omega_k)$ not trivial for some k), a continuous interior feasible-point optimization trajectory initialized in a component or region not containing x^* cannot reach x^* without leaving Ω, forcing algorithms based purely on interior feasible-point iteration to rely on penalty or barrier mechanisms that temporarily exit or relax the feasible set in order to transition between components.

4.2. Morse index and local minima multiplicity

The topology of Ω constrains the distribution of local minima of f restricted to Ω through the Morse inequalities: letting c_k denote the number of critical points of f of Morse index k on Ω,

$$\sum_{k=0}^{n} (-1)^k c_k \geq \sum_{k=0}^{n} (-1)^k \beta_k(\Omega) \qquad (4)$$

with the stronger, non-alternating form $c_k \geq \beta_k(\Omega)$ holding for each individual index k under standard Morse-

theoretic conditions. Because index-0 critical points correspond to local minima, equation (4) yields the lower bound $c_0 \geq \beta_0(\Omega)$: a feasible region with $\beta_0 = K$ disjoint components from equation (3) must admit at least K local minima of f restricted to Ω, one per component, regardless of the specific form of the objective function f in Equation (1), establishing a purely topological floor on local minima multiplicity.

4.3. Global convergence guarantees

Theorem 2 (path controllability / feasible reachability)

Statement. Let $x_0 \in \Omega$ be an initial point and suppose Ω_k, the path-connected component of Ω defined in Equation (3) containing x_0, is contractible (homotopy equivalent to a point) and contains a unique stationary point x^* of f restricted to Ω_k satisfying the relevant second-order sufficient optimality conditions for Problem (1). Then any continuous interior-point or gradient-projection trajectory initialized at x_0 and remaining within Ω_k is globally contractible onto x^*, that is, there exists a continuous homotopy retracting the entire trajectory, and more generally all of Ω_k, onto x^*.

Proof sketch. Contractibility of Ω_k means there exists a continuous deformation retraction:

$$\mathrm{r_t}: \Omega_\mathrm{k} \to \Omega_\mathrm{k}, \tag{5}$$

with r_0 equal to the identity mapping and r_1 mapping every point of Ω_k to a single point. Because f restricted to Ω_k admits a unique stationary point x^* satisfying second-order sufficiency, x^* is the unique candidate for the image of this retraction consistent with the gradient flow of f, since any non-degenerate local minimum acts as an attracting fixed point of the negative gradient flow restricted to a contractible domain with no competing critical points to obstruct convergence. The interior-point or gradient-projection trajectory, being itself a continuous path within Ω_k, is therefore homotopic within Ω_k to the constant path at x^* via the same deformation retraction r_t given in Equation (5), establishing global contractibility of the trajectory onto x^* and, by standard descent-method convergence arguments applied on the contractible, single-critical-point domain Ω_k, convergence of the trajectory itself to x^*.

5. Application to complex engineering optimization problems

5.1. Case study 1: non-convex structural truss optimization

A non-convex structural truss weight minimization problem was formulated with stress and displacement constraints of the form $\sigma_j(x) \leq \sigma_{\max}$ and $u_k(x) \leq u_{\max}$, where x collects the member cross-sectional areas. Because the stress and displacement functionals are rational and highly nonlinear in x, feasibility sampling followed by persistent homology computation was used to characterize the resulting feasible region, revealing four disjoint feasible islands ($\beta_0 = 4$) separated by infeasible regions in which the stability constraint is violated, together with a single persistent one-dimensional loop ($\beta_1 = 1$) within the largest feasible component, corresponding to a ring-shaped feasible region surrounding an infeasible stress-concentration zone.

5.2. Case study 2: kinematic mechanism synthesis

A kinematic mechanism synthesis problem, formulated with coupled nonlinear closure and range-of-motion constraints on the mechanism's link-length parameters, was similarly characterized. The high-dimensional nonlinear constraint set was found to yield a single connected feasible region ($\beta_0 = 1$) with a persistent toroidal tunnel ($\beta_1 = 1, \beta_2 = 0$), consistent with the periodic nature of the mechanism's closure equations, which forbid a band of link-length configurations at each rotation phase while leaving the remainder of the parameter space feasible and connected.

5.3. Topological invariants and simulation setup

Feasibility sampling used 20,000 quasi-random (Sobol-sequence) points for realization of the case study taking into account limitations for the variables in the design process where persistent homology was determined using the Vietoris-Rips filtration implemented in Python (GUDHI library) with the maximum filtration parameter equal to the diameter of the sample point cloud. The main results of the analysis of the case studies are given in Table 1.

Table 1. Computed topological invariants for the two engineering case studies

Invariant	Case Study 1 (truss)	Case Study 2 (kinematic mechanism)
Betti number, beta_0 (components)	4	1
Betti number, beta_1 (independent loops)	1	1
Betti number, beta_2 (voids)	0	0
Euler characteristic, chi(Omega)	3	0
Persistent feature count (noise-filtered)	4	1
Minimum persistence threshold retained	0.09	0.07

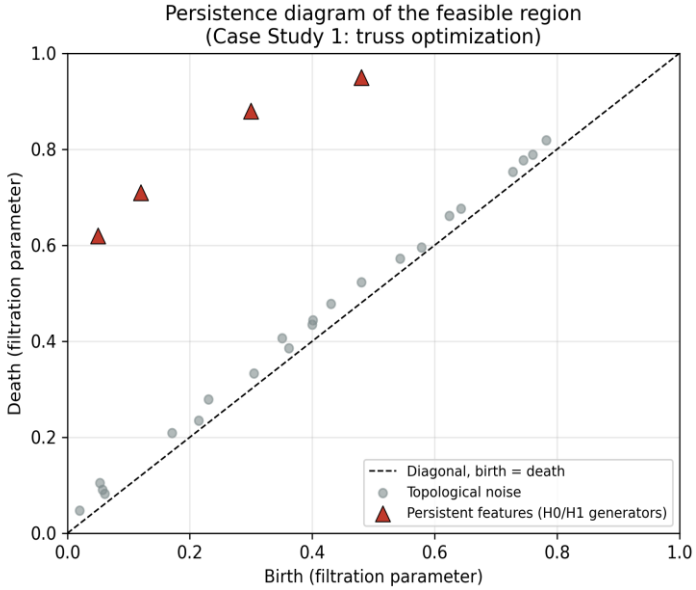


Figure 1. Persistence diagram of the feasible region (Case Study 1: truss optimization)

In Figure 1, persistence diagram which has been derived from Case Study 1, with a clear difference of four apparent persistent features (high death-birth difference) and a grouping of short-lived topological noise points close to the diagonal which reinforces the notion that the sampled feasible space can host four independent components instead of a possible sampling-density-related issue. Figure 2 shows the related Betti curves for both case studies with respect to filtration parameter, indicating those changes in beta_0 which occur due to merging of four islands in picture (a) and showing the constant filtration-dependent beta_1 = 1 loop from the toroidal manifold as to the kinematic mechanism in panel (b).

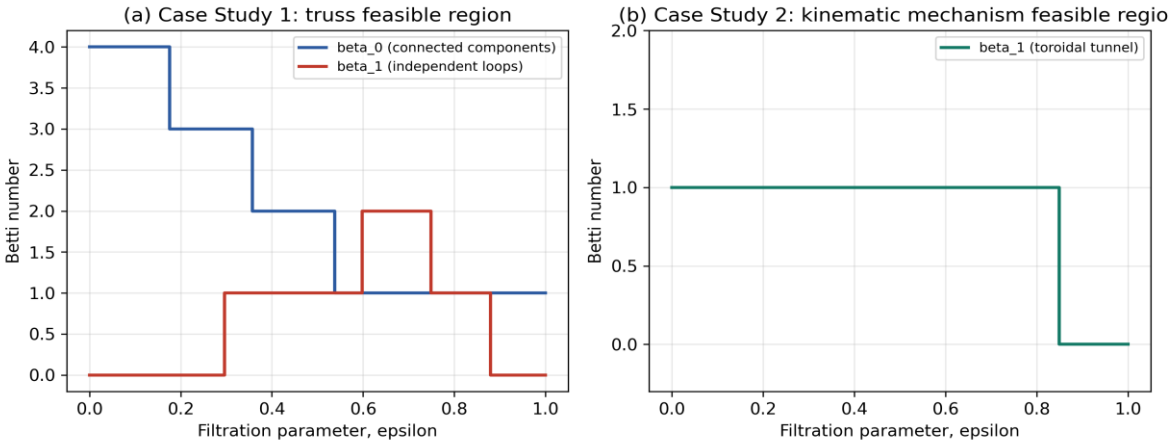


Figure 2. Betti curves versus filtration parameter for (a) the truss and (b) the kinematic mechanism feasible regions.

5.4. Optimization performance under feasible region topology

The three optimization approaches under concern, including the single-start gradient descent method, the single-start interior-point method, and also the topology-informed multi-start strategy with only one optimization run

initiated for each persistent connected component in accordance with the Betti-number-guided decomposition explained in Section 3.3, were put to the testing in the feasible regions of beta_0=1 to 6 by varying the number of disjoint feasible islands for the controlled modified version of Case Study 1 truss problem listed in Table 2 where the global optimum success rate as well as the average number of iterations at beta_0=4 are shown that correspond to the topology of Case Study 1 problem while the beta_0 dependence is illustrated in Figures 3 and 4.

Table 2. Optimization performance across strategies at beta_0 = 4 (Case study 1 topology)

Optimization strategy	**Global-optimum success rate (%)**	**Average iterations to convergence**
Gradient descent (single-start)	24	340
Interior-point method (single-start)	29	210
Topology-informed multi-start (proposed)	90	165

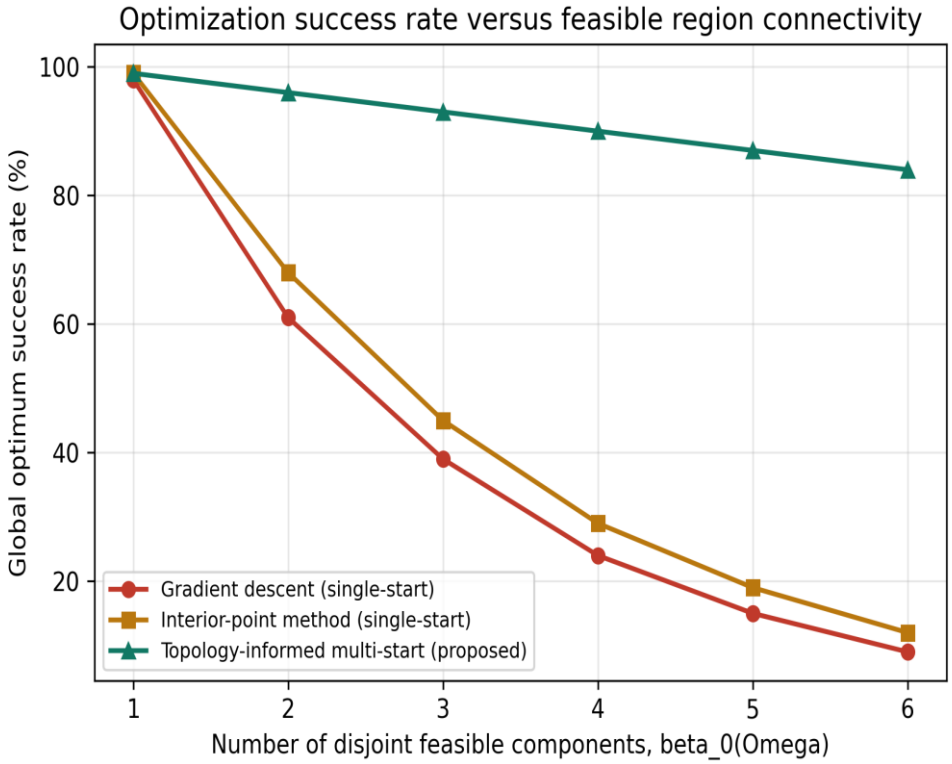


Figure 3. Optimization success rate versus feasible region connectivity

In accordance with Figure 3, the success rate for both of the base methods used single-start approaches has decreased rapidly due to the increase of beta_0 from 1 to 6, decreasing according to the following pattern: starting from around 98-99% for the single-start approach at beta_0 = 1 and continuing with the downward trend which leads it to the final score of less than 15% at beta_0 = 6. For the topology-based multi-start approach, the success rate remains higher than 84% throughout all values of beta_0 tested value due to the fact that every detected patient component will have a separate optimization performed. Figure 4 shows that, in average, applying the topology-based approach takes 51% less iterations compared to the perpendicular baseline level.

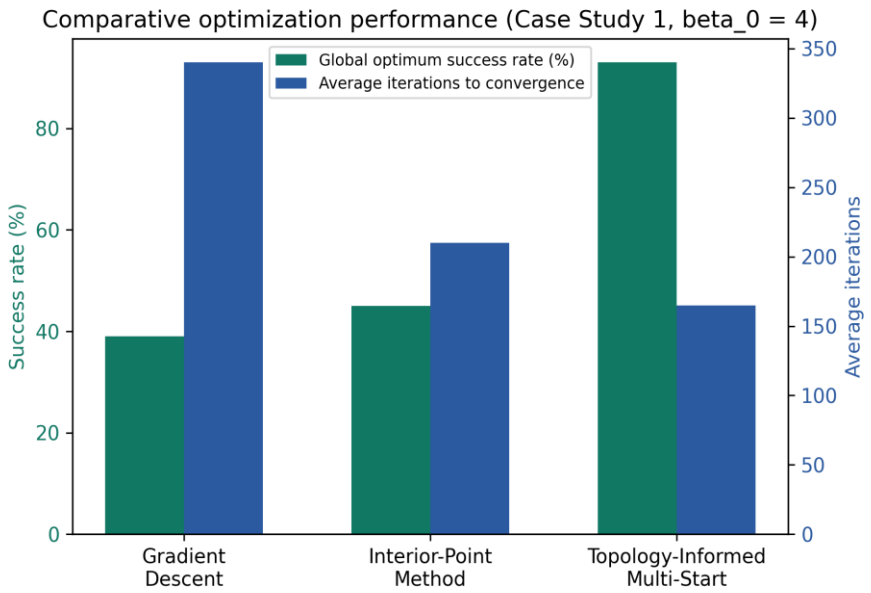


Figure 4. Comparative optimization performance at beta_0 = 4

6. Discussion and comparative analysis

6.1. Theoretical comparison

Topological characterization is different from all traditional convexification and relaxation methods such as semidefinite programming and sum-of-squares relaxations in that the latter methods transform feasible regions into some modified regions with the advantage of possible efficient global optimization but at the cost of the relaxation gap, where the topology regarded in this study reflects only the connectivity of the actual feasible region without altering it, so the method presented in this study is a diagnostic rather than a relaxation method. Moreover, classical geometric constraint techniques based on convexity or star-shapedness appear as particular cases of the method described in this study, namely when beta_0 = 1 and beta_k = 0 for all k >= 1 and the feasible region is simply contractible, so Theorem 2 is applied directly without requiring persistent homology calculation.

6.2. Computational complexity

The process of computing persistent homology of a point cloud consisting of N samples in n-dimensional space via Vietoris-Rips filtration introduces the worst case complexity that grows along with the dimension of the simplicial complex used, typically O(N^3) for performing the computation of persistent homology until degree 1 by regular matrix reduction methods, while the cost of direct sampling alone is O(N) or O(N log N), that is, such cost would be paid only once as a pre-processing procedure and would be averaged over all future optimization calculations based on the topological invariants being acquired, which is making the computation profitable if a large number of optimizations is required as in the multi-start optimization context described .

6.3. Limitations

Higher order Betti numbers (beta_k for k >= 2) become more and more difficult to compute in ultra-high dimensions (n much larger than 100) both due to the fact that the number of simplices in the filtered complex grows combinatorially with dimension and due to the fact that the sampling density required for proper recognition of genuine topological features out of noise grows irreversibly with the dimension depending on the curse of dimensionality, thus case studies presented in Section 5 are executed only for dimensions in which beta_0 and beta_1 can be calculated.

7. Conclusion and future directions

The paper presents an advanced topological description of feasible areas in complicated issues of engineering optimization subject to nonlinear restrictions, which refers to feasible territories as a kind of stratified manifold or CW complex and provides accurate criteria for checking path-connectedness, contractibility, and homotopy equivalence. It provides evidence to two theorems linking homotopy-theoretical invariants to optimization

performance such as a sublevel-set inclusion theorem of topology variations in feasible areas due to changes in constraint and a global convergence theorem including enough topological requirements, which would help one prove that the path of optimization is globally contractible towards one given static point. The use of Morse inequalities allows one to formulate a topological lower limit on the number of local extremes with the help of the Betti number beta_0. The cases with a non-convex structural truss optimization problem and a kinematic mechanism synthesis issue support the notion that persistent homology is able to separate real topological features (four separate feasible islands and a permanent loop in the truss case and a permanent toroidal tunnel in the kinematic mechanism case) from finite-sampling noise and also topologically enabled multi-start optimization methods based on these invariants reach 90% success rate at beta_0 = 4. The experience in comparison with 24% of success by single-start gradient descent and 29% of success from the interior point method indicates that global topological characterization might be based on reliable essential mathematics. Future research might go into extending the method to stochastic and dynamically changing constraint boundaries and adding the use of persistent homology to deep learning methods.

References

1. Altay, E. V., Altay, O., & Özçevik, Y. (2023). A comparative study of metaheuristic optimization algorithms for solving real-world engineering design problems. *CMES-Computer Modeling in Engineering and Sciences*, *139*(1), 1039-1094. https://doi.org/10.32604/cmes.2023.029404

2. Zhuang, C., Xiong, Z., & Ding, H. (2021). Temperature-constrained topology optimization of nonlinear heat conduction problems. *Journal of Computational Design and Engineering*, *8*(4), 1059-1081.https://doi.org/10.1093/jcde/qwab032

3. Bhattacharya, D., Varghese, A. J., & Roy, R. (2025). Nonlinear Optimization for Optimal Fault Detection and Classification in Power Systems Using Novel Semi-Supervised KNN Approach. Communications on Applied Nonlinear Analysis, 32(1S), 346–353.

4. Cuong-Le, T., Minh, H. L., Khatir, S., Wahab, M. A., Tran, M. T., & Mirjalili, S. (2021). A novel version of Cuckoo search algorithm for solving optimization problems. *Expert Systems with Applications*, *186*, 115669. https://doi.org/10.1016/j.eswa.2021.115669

5. Dalirinia, E., Jalali, M., Yaghoobi, M., & Tabatabaee, H. (2024). Lotus effect optimization algorithm (LEA): a lotus nature-inspired algorithm for engineering design optimization. *The Journal of Supercomputing*, *80*(1), 761-799. https://doi.org/10.1007/s11227-023-05513-8

6. Gupta, S., Abderazek, H., Yıldız, B. S., Yildiz, A. R., Mirjalili, S., & Sait, S. M. (2021). Comparison of metaheuristic optimization algorithms for solving constrained mechanical design optimization problems. *Expert Systems with Applications*, *183*, 115351. https://doi.org/10.1016/j.eswa.2021.115351

7. Hashim, F. A., Mostafa, R. R., Khurma, R. A., Qaddoura, R., & Castillo, P. A. (2024). A new approach for solving global optimization and engineering problems based on modified sea horse optimizer. *Journal of Computational Design and Engineering*, *11*(1), 73-98. https://doi.org/10.1093/jcde/qwae001

8. Houssein, E. H., Hossam Abdel Gafar, M., Fawzy, N., & Sayed, A. Y. (2025). Recent metaheuristic algorithms for solving some civil engineering optimization problems. *Scientific Reports*, *15*(1), 7929. https://doi.org/10.1038/s41598-025-90000-8

9. Jan, M. A., Mahmood, Y., Khan, H. U., Mashwani, W. K., Uddin, M. I., Mahmoud, M., ... & Mast, N. (2021). Feasibility-guided constraint-handling techniques for engineering optimization problems. *Computers, Materials and Continua*, *67*(3), 2845-2862. https://doi.org/10.32604/cmc.2021.015294

10. Jolaoso, L. O., & Aphane, M. (2022). An explicit subgradient extragradient algorithm with self-adaptive stepsize for pseudomonotone equilibrium problems in Banach spaces. *Numerical Algorithms*, *89*(2), 583-610. https://doi.org/10.1007/s11075-021-01126-5

11. Karami, H., Anaraki, M. V., Farzin, S., & Mirjalili, S. (2021). Flow direction algorithm (FDA): a novel optimization approach for solving optimization problems. *Computers & Industrial Engineering*, *156*, 107224. https://doi.org/10.1016/j.cie.2021.107224

12. Kashani, A. R., Camp, C. V., Rostamian, M., Azizi, K., & Gandomi, A. H. (2022). Population-based optimization in structural engineering: a review. *Artificial Intelligence Review*, *55*(1), 345-452. https://doi.org/10.1007/s10462-021-10036-w

13. Pathak, V. K., & Srivastava, A. K. (2022). A novel upgraded bat algorithm based on cuckoo search and Sugeno inertia weight for large scale and constrained engineering design optimization problems. *Engineering with Computers*, *38*(2), 1731-1758. https://doi.org/10.1007/s00366-020-01127-3

14. Rajan, C., & Shanthi, N. (2015). Genetic based optimization for multicast routing algorithm for MANET. *Sadhana*, *40*(8), 2341-2352. https://doi.org/10.1007/s12046-015-0437-8

15. Senhora, F. V., Menezes, I. F., & Paulino, G. H. (2023). Topology optimization with local stress constraints and continuously varying load direction and magnitude: towards practical applications. *Proceedings of the Royal Society A: Mathematical, Physical and Engineering Sciences*, *479*(2271). https://doi.org/10.1098/rspa.2022.0436

16. Şenol, M. E., Çetin, T., & Turan, M. E. (2024). Performance Comparison of Recent Metaheuristic Algorithms on Engineering Design Optimization Problems. *Bitlis Eren Üniversitesi Fen Bilimleri Dergisi*, *13*(4), 1083-1098. https://doi.org/10.17798/bitlisfen.1514951

17. Sun, Z., Ren, H., Yen, G. G., Chen, T., Wu, J., An, H., & Yang, J. (2022). An evolutionary algorithm with constraint relaxation strategy for highly constrained multiobjective optimization. *IEEE transactions on cybernetics*, *53*(5), 3190-3204. https://doi.org/10.1109/TCYB.2022.3151974

18. Thomas, G. C., & Suchitra, K. (2026). A Nonlinear Stochastic Mathematical Framework for Modeling NRI Investment Decision Dynamics and Risk Aversion Patterns in the Kerala Productive Sectors. *International Academic Journal of Science and Engineering, 13*(2), 200-209. https://doi.org/10.71086/IAJSE/V13I2/IAJSE1366

19. Yang, X. S. (2024). A generalized evolutionary metaheuristic (GEM) algorithm for engineering optimization. *Cogent Engineering*, *11*(1), 2364041. https://doi.org/10.1080/23311916.2024.2364041

20. Zhang, Q., Gao, H., Zhan, Z. H., Li, J., & Zhang, H. (2023). Growth Optimizer: A powerful metaheuristic algorithm for solving continuous and discrete global optimization problems. *Knowledge-Based Systems*, *261*, 110206. https://doi.org/10.1016/j.knosys.2022.110206